

FAST TRACK COMMUNICATION

Sodium sulfate heptahydrate: direct observation of crystallization in a porous material

Andrea Hamilton^{1,3}, Christopher Hall¹ and Leo Pel²¹ School of Engineering and Electronics and Centre for Materials Science and Engineering, The University of Edinburgh, The King's Buildings, Edinburgh EH9 3JL, UK² Department of Applied Physics, Eindhoven University of Technology, PO Box 513, 5600 MB Eindhoven, The NetherlandsE-mail: andrea.hamilton@ed.ac.uk

Received 16 June 2008, in final form 22 August 2008

Published 15 October 2008

Online at stacks.iop.org/JPhysD/41/212002

Abstract

It is well known that sodium sulfate causes salt crystallization damage in building materials and rocks. However since the early 1900s the existence of the metastable heptahydrate has been largely forgotten and almost entirely overlooked in scientific publications on salt damage mechanics and on terrestrial and planetary geochemistry. We use hard synchrotron x-rays to detect the formation of this metastable heptahydrate on cooling a porous calcium silicate material saturated with sodium sulfate solution. The heptahydrate persists indefinitely and transforms to mirabilite only below 0 °C. At the transformation, which is rapid, the solution is highly supersaturated with respect to mirabilite. We estimate that crystallization of the heptahydrate and of mirabilite have associated Correns pressures of about 9 and 19 MPa, respectively, exceeding the tensile strength of building stones. We detect lattice strains in the salts from x-ray measurements consistent with these values.

(Some figures in this article are in colour only in the electronic version)

1. Introduction

Hydrated sodium sulfate causes salt crystallization damage in building materials and rocks [1], and is found in Antarctic ice [2], and in salt lakes [3]. Landform alteration is the result of salt weathering on Earth and probably on Mars [4]. The well-known sodium sulfate decahydrate $\text{Na}_2\text{SO}_4 \cdot 10\text{H}_2\text{O}$, *mirabilite*, is thought to form in the icy brines on the moons of Jupiter [5, 6]. In stone decay in buildings and archaeological sites, sodium sulfate is regarded as particularly damaging, probably because this salt can easily form a solution which is highly supersaturated with respect to mirabilite [7]. Correns showed that a salt in contact with its supersaturated solution can produce a *crystallization pressure* [8, 9] in a host matrix [10]. However many questions remain about the

destructive nature of sodium sulfate [11], not least because of the absence of direct evidence that mirabilite forms in building stones and porous rocks. Now, using hard synchrotron x-rays to obtain *in situ* powder diffraction patterns [12] we observe directly a salt crystallization sequence within a porous matrix on cooling. We have used quantitative ²³Na NMR independently to monitor the salt concentration in the solution [13]. Cooling aqueous sodium sulfate solutions in a high porosity calcium silicate material [14, 15], we find that the salt first formed on cooling is not mirabilite but the metastable hydrate $\text{Na}_2\text{SO}_4 \cdot 7\text{H}_2\text{O}$ [16], a crystal of which is shown in figure 1. Although it is invariably assumed that mirabilite is the salt formed in salt damage processes, the early scientific literature contains several extensive studies of the metastable heptahydrate [16, 17]. These show that the heptahydrate is almost always the first hydrate to crystallize from supersaturated sodium sulfate solutions on cooling, and

³ Author to whom any correspondence should be addressed.

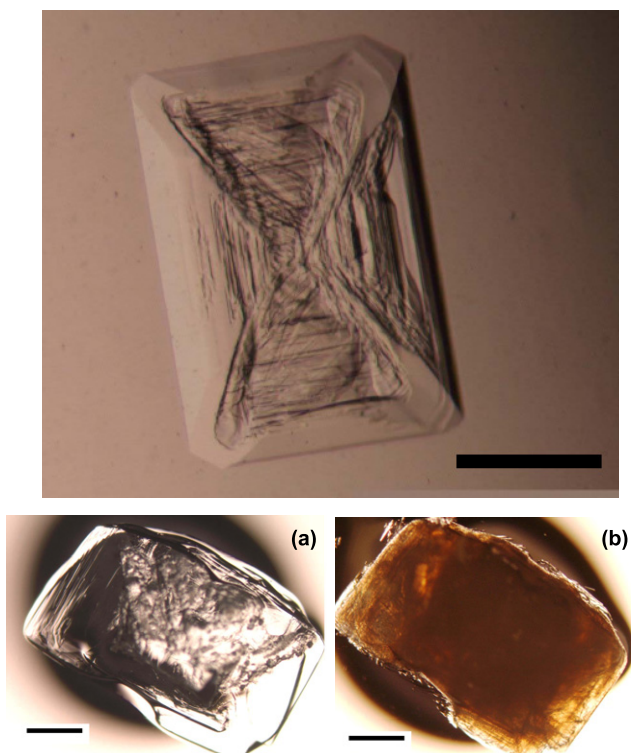


Figure 1. (Top) A crystal of sodium sulfate heptahydrate grown by cooling a 3.4 m Na_2SO_4 aqueous solution on an ice bath. Scale bar 600 μm . (Bottom) A heptahydrate crystal in mineral oil (a) before and (b) after pseudomorphic transformation to mirabilite caused by momentary contact with a seed crystal. The transformed crystal is strongly opaque and noticeably textured. Scale bars 1 mm.

that mirabilite forms only with difficulty. The nineteenth and early twentieth century scientific literature contrasts sharply with the more recent literature in emphasizing the prominence of the heptahydrate.

2. Experiments

All experiments were carried out on cylindrical plugs of hydrated calcium silicate 22 mm diameter \times 45 mm long, a construction material chosen for its high porosity (volume fraction porosity of 0.90 and mean pore radius 0.33 μm) and composed mainly of elongated particles of xonotlite [14, 15]. The cores were capillary saturated with 3.4 molal (m) sodium sulfate solution and either encased in a PE sleeve (x-ray measurements) or wrapped in hydrophobic PTFE tape (NMR measurements) to prevent evaporation. The 3.4 m concentration used is close to the solubility of thenardite at 30–40 $^\circ\text{C}$, and typical of the more concentrated solutions formed by taking up water into stones which have previously deposited thenardite by evaporation.

X-ray data were obtained on beamline 16.4 at the UK Synchrotron Radiation Source, Daresbury. Plug and sleeve were mounted vertically in a thermostatted cooling block, and rotated about the cylinder axis. The sample temperature was estimated from the measured temperature of the cooling block by applying Newton's law of cooling. A collimated beam of polychromatic x-rays passed through the sample and Bragg scattered x-rays were intercepted at fixed scattering angles

by a bank of three energy-dispersive Ge detectors [18]. The sample holder was cooled from 48 to -15°C over 172 min. The powder diffraction reference pattern of the heptahydrate was obtained in a separate series of experiments using the same synchrotron instrumentation [12]. Replicate calcium silicate plugs cooled at an overall cooling rate of 30°C h^{-1} were examined with time-resolved ^{23}Na NMR measurements of solution concentration using the method described by Rijniers *et al* [13].

3. Results

The *in situ* x-ray measurements we report provide the first direct evidence that heptahydrate nucleates in preference to mirabilite when a capillary saturated porous material is cooled. During cooling, the dissolved salt concentration in the porous material remains constant at first while the solution becomes increasingly supersaturated with respect to both mirabilite and heptahydrate as their solubilities fall. The x-ray sample temperature was estimated from ^{23}Na NMR experiments which showed (indirectly) that heptahydrate crystallizes reproducibly at 10 $^\circ\text{C}$ in saturated calcium silicate cores when cooled at a rate of around 30°C h^{-1} . We calculate the cooling rate of the samples in the x-ray experiments by applying Newton's cooling law to the measured cooling rate of the temperature-controlled sample block, knowing the initial sample temperature and assuming that heptahydrate precipitation occurs at 10 $^\circ\text{C}$. From this analysis we calculate an overall sample cooling rate of around 22°C h^{-1} from the start of the experiment to heptahydrate precipitation, close to the NMR sample cooling rate of 30°C h^{-1} . NMR experiments suggest that the cooling rate would have to be decreased by at least an order of magnitude for the temperature of precipitation to rise by a few degrees centigrade. At a temperature which we estimate to be 10 $^\circ\text{C}$ we observe a spontaneous and sudden crystallization of sodium sulfate heptahydrate as shown by the changes in the XRD pattern (figure 2 (Left)). NMR data show that there is a sharp fall in sodium sulfate concentration in solution (figure 3) to a value close to the heptahydrate solubility (2.10 m). It is evident from figure 3 that on cooling the solution concentration is slightly higher than the equilibrium curve. The rate of crystallization depends on the cooling rate which is too rapid for equilibrium to be reached fully in the short time the system remains at each temperature. The equilibrium curve may be more closely followed with a slower cooling rate. At around -2°C , based on the calculated sample cooling rate, there is a dramatic change in the XRD pattern and a further fall in solution concentration as the heptahydrate transforms to mirabilite. This is in good agreement with the measured ^{23}Na NMR conversion temperature of around -4°C . The x-ray sample is cooled to an estimated final temperature of -6°C and we do not detect the formation of ice. We find in general that heptahydrate shows a greater tendency to convert to mirabilite at temperatures around or below 0 $^\circ\text{C}$.

Using the 103 reflection of heptahydrate and the 002 reflection of mirabilite, we can follow the transformation kinetics (figure 2 (Right)). The nucleation and initial rapid crystal growth of the heptahydrate occur over about 7 min;

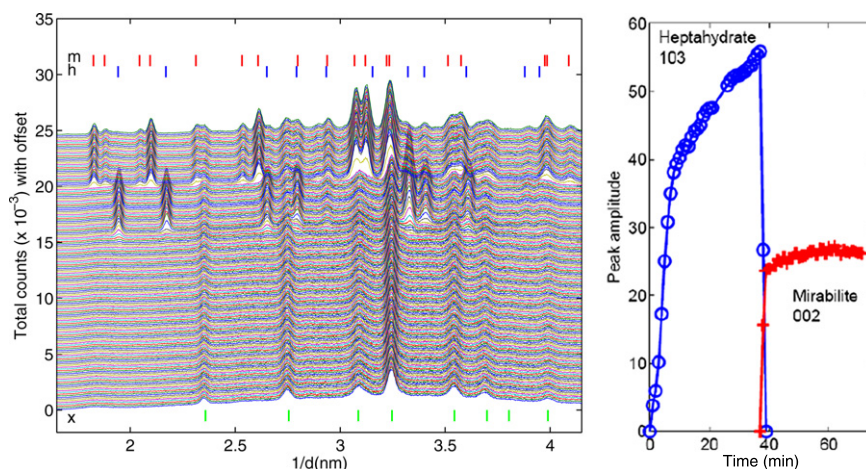


Figure 2. (Left) Energy-dispersive x-ray diffraction patterns obtained during cooling of a cylindrical calcium silicate core saturated with a 3.4 m sodium sulfate solution. Patterns were recorded every 30 s from a starting sample temperature of 48 °C and show precipitation of heptahydrate at 10 °C and mirabilite at −2 °C. Markers show expected positions of the main diffraction peaks of xonotlite (x), the main mineral phase of the calcium silicate core (JCPDS card 23-125); of heptahydrate (h) [12]; and of mirabilite (m) (JCPDS card 75-1077). (Right) Growth of the heptahydrate 103 reflection (○) and of the mirabilite 002 (+) reflection from synchrotron x-ray diffraction data.

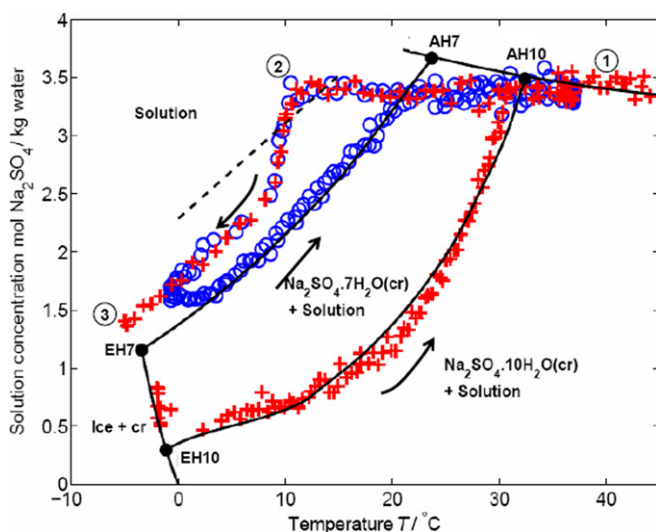


Figure 3. Dissolved salt concentrations obtained by ^{23}Na NMR measurements on calcium silicate cores saturated with 3.4 m aqueous sodium sulfate solution. Experimental data from two cooling/heating runs are superimposed on the $\text{Na}_2\text{SO}_4\text{-H}_2\text{O}$ phase diagram defined by solubility curves (solid lines) for mirabilite, heptahydrate, thenardite and ice. The dotted line shows the supersolubility curve for heptahydrate [16], an approximate upper bound on the supersaturation which can be maintained before crystallization occurs. EH10 and EH7 are the eutectic points for heptahydrate–ice and mirabilite–ice; AH7 is the co-existence point for heptahydrate–thenardite; and AH10 that for mirabilite–thenardite. (1) marks the start of a cooling experiment, (2) the crystallization of heptahydrate and (3) the crystallization of mirabilite. Points ○: data obtained on cooling at 30 °C h⁻¹ from 40 °C to a minimum temperature of 0 °C showing heptahydrate crystallization occurring at about 10 °C; on reheating, the solution concentration follows the heptahydrate solubility curve. Points +: data on cooling at 30 °C h⁻¹ to a minimum temperature of −4 °C, where heptahydrate transforms to mirabilite and the solution concentration decreases to lie on the mirabilite solubility curve. On reheating, the solution follows the mirabilite solubility curve.

thereafter there is a slow increase in the intensity of the 1 0 3 and other diffraction peaks as cooling continues. The 30% increase in mass of crystals corresponds to the decrease in solubility of heptahydrate with temperature. After the initial crystallization heptahydrate crystals occupy 28% of the pore space; this increases to 41% as the sample cools to about −2 °C. The transformation of heptahydrate to mirabilite is spectacularly fast, and is complete in less than 2 min. In the fully transformed system at −2 °C, we calculate from solubility data [19] that 64% of the pore volume is occupied by solid mirabilite in equilibrium with saturated sodium sulfate solution (0.27 m Na_2SO_4). Once nucleated, crystal growth of mirabilite is evidently rapid. As mirabilite is considerably less soluble than the heptahydrate, strong concentration gradients drive ion diffusion through solution towards the growing mirabilite crystals. Mirabilite and heptahydrate have different crystal structures, but mirabilite crystals grow in close proximity to pre-existing heptahydrate in a system which contains little solution. Under the microscope, we see a rapid pseudomorphic replacement of heptahydrate by mirabilite, and something similar undoubtedly occurs in the confined pore space which also contains rather little solution.

Careful analysis of x-ray diffraction peak shifts provides direct evidence of lattice strain in the salt hydrate crystals as they grow and are confined by the matrix on which they exert increasing stress. Lattice strain estimates were obtained by Gaussian fitting to selected diffraction peaks. This provides accurate values of changes in d -spacing, and hence strain, within sequences of diffraction patterns obtained during a single cooling run. Observed strains were corrected for the effects of thermal contraction. In figure 4 we show the compressive deformation of the hydrate lattice during the crystallization process of figure 2. The d -spacing shifts of selected peaks show that (after correcting for thermal contraction) the heptahydrate develops only a small linear compressive strain of not more than about 1×10^{-4} during crystallization, but the mirabilite shows a larger compressive

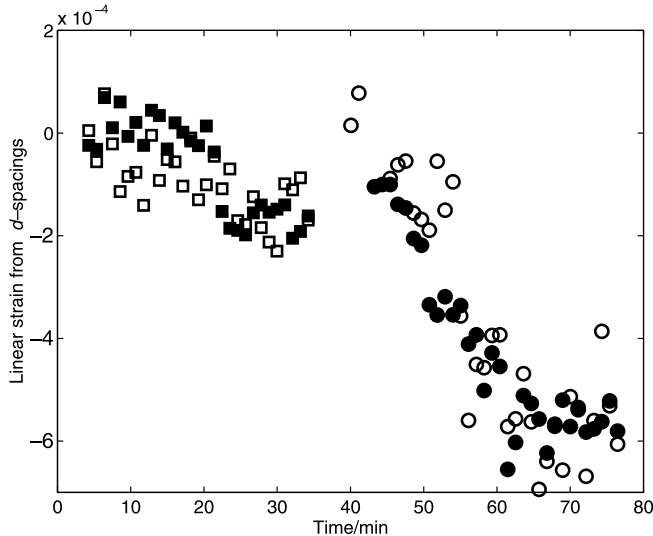


Figure 4. Estimated lattice strains calculated from shifts in d -spacings in heptahydrate and mirabilite during salt crystallization. ■ heptahydrate 105, □ heptahydrate 204 reflections, ● mirabilite 002, ○ mirabilite 223 peaks. Data are corrected for the effects of thermal contraction due to cooling. Zero strain is taken at the beginning of crystallization for each hydrate.

lattice strain of about 5.5×10^{-4} (figure 4.) The compressive strain in mirabilite rises rapidly at first and then stabilizes. We assume an approximate bulk modulus of 20 GPa for both hydrates, based on values measured for two other salt hydrates, ikaite and epsomite [20, 21]. We then calculate from the observed lattice strains that the compressive stress in the heptahydrate cannot be more than about 2 MPa but in the mirabilite it is about 11 MPa. It should be noted that the calcium silicate matrix used here is a rather unusual porous material, which consists of a loose network of acicular crystals rather than a conventional pore system in a solid matrix. What we present is a novel way of extracting some information on the strain experienced by salt crystals inside a porous matrix.

4. Discussion

A link between these phenomena and damage mechanics lies in the Correns equation for crystallization pressure [8], recently reworked by Flatt [9], Coussy [22] and Steiger [23]. The Correns pressure ΔP in the form derived by Steiger is given by equation (1):

$$\Delta P = \frac{\nu RT}{V_m} \left(\ln \frac{m}{m_0} + \ln \frac{\gamma_{\pm}}{\gamma_{\pm,0}} + \frac{\nu_w}{\nu} \ln \frac{a_w}{a_{w,0}} \right), \quad (1)$$

where γ_{\pm} is the mean ion activity, m is the concentration of the solution in moles per kg water and a_w is the activity of water. Subscript zero indicates a value before crystallization takes place. ν_w is the number of water molecules combined in the hydrate, ν the stoichiometric number for the ions, V_m the molar volume of the salt, R the gas constant and T the absolute temperature. The Correns pressure is the maximum pressure that a salt crystal growing in a supersaturated solution can exert on the pore wall provided this does not exceed the disjoining

pressure associated with the salt crystal-pore wall contact. As is evident, high supersaturations are essential for generating large stresses. Our results allow us to establish conclusively the identity of the precipitating phase in a porous material, to quantify the supersaturations and also to carry out complete mass and volume balances. It is assumed that a crystal makes contact with the pore wall though a film of solution so that growth can be maintained [10]. Pitzer water and ion activities have been calculated using FREZCHEM [24]. Supersaturations from +15 to -5°C were estimated from heptahydrate solubility data [25]. A fixed pre-crystallization solution concentration of 3.41 m was used, corresponding to our experimental system. The solubility product of heptahydrate in the temperature range 0 – 25°C and 1 atm pressure calculated from solubility data over the temperature range 0 – 23.7°C is $\ln K_{sp} = -45.72755 + 0.2126744T - 2.176074 \times 10^{-4}T^2$ with T the absolute temperature [26]. In our case the solution reaches a supersaturation m/m_0 with respect to heptahydrate of 1.6 at 10°C with a calculated crystallization pressure of about 8.8 MPa. The Correns pressure increases rapidly as nucleation temperature falls, primarily because the supersaturation with respect to the heptahydrate solid phase increases.

Just before mirabilite forms at about -2°C the supersaturation with respect to mirabilite is 3.9 and the calculated Correns pressure P is 19.2 MPa. These Correns pressures, which set upper bounds on the real stress in the salt crystals, are consistent with our estimates of compressive stress from the observed lattice strains which are lower. The effective stress in the matrix is to a first approximation ϕP where ϕ is the volume fraction of solid hydrate in bulk material. From this, we estimate that the bulk stress on crystallization of heptahydrate at 10°C cannot be greater than about 2.2 MPa; and on crystallization of mirabilite at -2°C cannot exceed about 11 MPa. Indeed applying ϕP to the compressive stress calculated from the observed lattice strains we estimate that the actual stresses in the matrix are 0.5 MPa and 6.3 MPa for heptahydrate crystallization at 10°C and mirabilite at -2°C , respectively. These values sit below the upper bound stresses in the matrix as calculated from the Correns pressure. Stress transfer to the matrix is of course complex since there are both equilibrium and non-equilibrium processes at work and the coupling of solubility to stress ensures that stress relaxation must occur. In equilibrium situations crystals present in the matrix are in equilibrium with the surrounding pore solution. Non-equilibrium effects [7, 27] are the result of continued crystal growth from a supersaturated solution (generally requiring long range diffusive transport of ions to the growing crystal to sustain) leading to the development of the Correns crystallization pressure. In practice some combination of both may occur. It appears that the strong crystallization pressures developed in materials saturated with sodium sulphate solution are primarily the result of the difficulty of nucleating mirabilite.

5. Conclusions

Our results show that heptahydrate is the first sodium sulfate hydrate to form in a calcium silicate porous matrix on cooling and only converts to mirabilite at temperatures

below about 0°C. (There is indirect evidence also for heptahydrate formation limestones [28]). We also quantify the supersaturation attainable in a closed system before crystallization. This allows us to calculate with more accuracy the maximum (limiting) Correns pressure, and the amounts of solid salts formed and the volumes and compositions of the solution at every stage. From the analysis of diffraction peak positions we are able to investigate the strain imposed on the crystals by the matrix and compare the corresponding stress with these calculated Correns pressures. We conclude that the sudden burst of mirabilite crystallization at low temperatures and associated strain produced sheds new light on the ability of sodium sulfate to damage porous materials. Finally we note that sodium sulfate heptahydrate may be of much wider significance. Gans [29] in his work on the water vapour pressure–temperature phase diagram finds a region of stability for the otherwise metastable heptahydrate at sub-zero temperatures and low relative humidity values. Extrapolating this phase diagram to the conditions of the surface of Mars suggests that heptahydrate formation on Mars is possible [26]. Given the reluctance of mirabilite to nucleate directly from solution, our results also suggest the possibility that heptahydrate as well as mirabilite may occur in salt playas and lakes on Earth, in Antarctic ice and on Jupiter's icy moons [26].

Acknowledgments

We thank EPSRC for research funding; David Taylor, SRS, Daresbury Laboratory, UK for synchrotron support; a part of this project was supported by the Dutch Technology Foundation (STW).

References

- [1] Goudie A S and Viles H A 1997 *Salt Weathering Hazards* (Chichester, UK: Wiley)
- [2] Ohno H, Igarashi M and Hondoh T 2006 *Geophys. Res. Lett.* **33** L08501
- [3] Sack L A and Last W M 1994 *J. Paleolimnol.* **10** 199
- [4] Jagoutz E 2006 *Adv. Space Res.* **38** 696
- [5] Kargel J S, Kaye J Z, Head J W, Marion G M, Sassen R, Crowley J K, Ballesteros O P, Grant S A and Hogenboom D L 2000 *Icarus* **148** 226
- [6] Marion G M, Kargel J S, Caitling D C and Jakubowski S D 2005 *Geochim. Cosmochim. Acta* **69** 259
- [7] Flatt R J 2002 *J. Cryst. Growth* **242** 435
- [8] Correns C W 1949 *Discuss. Faraday Soc.* **5** 267
- [9] Flatt R J, Scherer G W and Steiger M 2007 *Environ. Geol. Lett.* **52** 187
- [10] Scherer G W 1999 *Cem. Concr. Res.* **29** 1347
- [11] Rodriguez-Navarro C and Doehne E 1999 *Earth Surf. Process. Landf.* **24** 191
- [12] Hamilton A and Hall C 2008 *J. Anal. At. Spectrom.* **23** 840
- [13] Rijniers L A, Huinink H, Pel L and Kopinga K 2005 *Phys. Rev. Lett.* **94** 075503
- [14] Hamilton A and Hall C 2005 *J. Build. Phys.* **29** 9
- [15] Hamilton A and Hall C 2007 *J. Build. Phys.* **31** 69
- [16] Hartley H, Jones B M and Hutchison G A 1908 *J. Chem. Soc.* **93** 825
- [17] Loewel H 1850 *Ann. Chim. Phys.* **29** 62
- [18] Barnes P *et al* 1998 *Nucl. Instrum. Methods B* **134** 310
- [19] Gmelin L 1961 *Gmelins Handbuch der Anorganischen Chemie Systeme Nr. 21, Natrium* (Verlag Chemie GmbH)
- [20] Lennie A R 2005 *Mineral. Mag.* **69** 325
- [21] Fortes A D, Wood I G, Alfredsson M, Vocadlo L and Knight K S 2006 *Eur. J. Mineral.* **18** 449
- [22] Coussy O 2006 *J. Mech. Phys. Solids* **54** 1517
- [23] Steiger M 2005 *J. Cryst. Growth* **282** 455
- [24] Marion G M and Kargel J S 2008 *Cold Aqueous Planetary Geochemistry with FREZCHEM* (Berlin/Heidelberg: Springer)
- [25] Eddy R D and Menzies A W C 1940 *J. Phys. Chem.* **44** 207
- [26] Hall C and Hamilton A 2008 *Icarus* doi:10.1016/j.icarus.2008.07.001
- [27] Scherer G W 2004 *Cem. Concr. Res.* **34** 1613
- [28] Rijniers L A 2005 *PhD Thesis* Technical University of Eindhoven, Netherlands
- [29] Gans W 1978 *Z. Phys. Chem.* **111** 39